Chapter 18
Magnetic Fields in Galaxies

Rainer Beck

Abstract The origin and evolution of cosmic magnetic fields, their strength and structure in intergalactic space, their first occurrence in young galaxies, and their dynamical importance for galaxy evolution remain widely unknown. Radio synchrotron emission, its polarization and its Faraday rotation are powerful tools to study the strength and structure of magnetic fields in galaxies. Unpolarized radio synchrotron emission traces isotropic turbulent fields which are strongest in spiral arms and bars (20–30 μG) and in central starburst regions (50–100 μG). Such fields are dynamically important; they can affect gas flows and drive gas inflows in central regions. Polarized radio emission traces ordered fields which can be regular or anisotropic turbulent, generated from isotropic turbulent fields by compression or shear. The strongest ordered fields of 10–15 μG strength are generally found in interarm regions and follow the orientation of adjacent gas spiral arms. In galaxies with strong density waves, ordered (anisotropic turbulent) fields are also observed at the inner edges of the spiral arms. Ordered fields with spiral patterns exist in grand-design, barred and flocculent galaxies, and in central regions of starburst galaxies. Ordered fields in interacting galaxies have asymmetric distributions and are an excellent tracer of past interactions between galaxies or with the intergalactic medium. Irregular galaxies host isotropic turbulent fields often of similar strength as in spiral galaxies, but only weak ordered fields. Faraday rotation measures (RM) of the diffuse polarized radio emission from the disks of several galaxies reveal large-scale spiral patterns that can be described by the superposition of azimuthal modes; these are signatures of regular fields generated by a mean-field $\alpha - \Omega$ dynamo. So far no indications were found in external galaxies of large-scale field reversals, like the one in the Milky Way. Ordered magnetic fields are also observed in radio halos around edge-on galaxies out to large distances from the plane, with X-shaped patterns. In the outflow cone above a starburst region of NGC 253, RM data indicate a helical magnetic field.

R. Beck (✉)
Max-Planck-Institut für Radioastronomie, Auf dem Hügel 69, 53121 Bonn, Germany
e-mail: rbeck@mpifr-bonn.mpg.de

A. Lazarian et al. (eds.), *Magnetic Fields in Diffuse Media*, Astrophysics and Space Science Library 407, DOI 10.1007/978-3-662-44625-6_18

18.1 Introduction

Magnetic fields are a major agent in the interstellar medium and control the density and distribution of cosmic rays. Cosmic rays accelerated in supernova remnants can provide the pressure to drive galactic outflows and buoyant loops of magnetic fields via the Parker instability. Outflows from starburst galaxies in the early Universe may have magnetized the intergalactic medium.

The detection with the AUGER observatory of ultrahigh-energy cosmic rays (UHECRs) reaching the Earth and the possibly anisotropic distribution of their arrival directions (Abreu 2010) calls for a proper model of particle propagation. As UHECR particles are deflected by large-scale regular fields and scattered by turbulent fields, the structure and the extent of the fields in the disk and halo of the Milky Way are necessary parameters for a propagation model, but our present knowledge does not allow safe conclusions. The view onto external spiral galaxies can help.

18.2 Origin of Magnetic Fields

The origin of the first magnetic fields in the Universe is a mystery (Widrow 2002). *Seed fields* may be "primordial", generated during a phase transition in the early Universe (Caprini et al. 2009), or may originate from the time of cosmological structure formation by the Weibel instability (Lazar et al. 2009), or from injection by the first stars or jets generated by the first black holes (Rees 2005), or from the Biermann mechanism in the first supernova remnants (Hanayama et al. 2005), or from plasma fluctuations (Schlickeiser 2012). The non-detection of GeV γ-ray emission with the FERMI satellite from blazars, which were observed at TeV energies with the HESS observatory, may indicate that the secondary particles are deflected by intergalactic fields of least 10^{-16} G strength and a high volume filling factor (Dolag et al. 2011).

The most promising mechanism to sustain magnetic fields in the interstellar medium of galaxies is the dynamo (Beck et al. 1996). A small-scale dynamo in protogalaxies may have amplified seed fields to several μG strength (the energy level of turbulence) within less than 10^8 year (Schleicher et al. 2010). To explain the generation of large-scale fields in galaxies, the mean-field $\alpha - \Omega$ dynamo has been developed. It is based on turbulence, differential rotation and helical gas flows (*α-effect*), driven by supernova explosions (Gressel et al. 2008). The $\alpha - \Omega$ dynamo generates large-scale helicity with a non-zero mean in each hemisphere. As total helicity is a conserved quantity, the dynamo is quenched by the small-scale fields with opposite helicity unless these are removed from the system (Shukurov et al. 2006). Outflows are essential for effective $\alpha - \Omega$ dynamo action. The mean-field approximation got support from high-resolution MHD modeling (Gent et al. 2013).

Dynamo-type fields are described by modes with different azimuthal symmetries in the disk plane and two different vertical symmetries (even or odd parity) perpendicular to the disk plane. Several modes can be excited in the same object. In flat, rotating objects like galaxy disks, the strongest mode S0 consists of a toroidal field of *axisymmetric spiral* shape within the disk, without sign reversals across the equatorial plane, and a weaker poloidal field of even-symmetry structure. The $\alpha-\Omega$ dynamo in galaxy disks predicts that within a few 10^9 year large-scale regular fields are generated from μG turbulent fields (Arshakian et al. 2009). Field reversals from the early phases may survive until today (Moss et al. 2012). Global numerical models of galaxies (Gissinger et al. 2009; Hanasz et al. 2009) confirmed the basic results of the $\alpha-\Omega$ dynamo. Dynamo modes can be identified observationally from the pattern of polarization angles and of RMs of the diffuse polarized emission of galaxy disks (see Sect. 18.6.1).

18.3 Measuring Magnetic Fields in Galaxies

Magnetic fields need illumination to be detectable. *Polarized emission* at optical, infrared, submillimeter and radio wavelengths holds the clue to measure magnetic fields in galaxies. Optical linear polarization is a result of extinction by elongated dust grains in the line of sight which are aligned in the interstellar magnetic field (the *Davis-Greenstein effect*). The B-vector (E + 90°) runs perpendicular to the field. Starlight polarization yields the orientation of large-scale magnetic fields in the Milky Way (Fosalba et al. 2002). However, light can also be polarized by scattering, a process unrelated to magnetic fields and hence a contamination that is difficult to subtract from diffuse polarized emission from galaxies, e.g. in the spiral galaxy M 51 (Scarrott et al. 1987).

Linearly polarized emission from elongated dust grains at infrared and submillimeter wavelengths is not affected by polarized scattered light. The B-vector is parallel to the magnetic field. The field structure can be mapped in gas clouds of the Milky Way and in galaxies, e.g. in the halo of the galaxy M 82 (Greaves et al. 2000).

Most of what we know about interstellar magnetic fields comes through the detection of radio waves. *Zeeman splitting* of radio spectral lines directly measures the field strength in gas clouds of the Milky Way (Crutcher et al. 2010) and in starburst galaxies (Robishaw et al. 2008). The intensity of *synchrotron emission* (Chap. 3; examples in Figs. 18.1 and 18.5) is a measure of the number density of cosmic-ray electrons in the relevant energy range and of the strength of the total magnetic field component in the sky plane. The assumption of energy equipartition between these two components allows us to calculate the total magnetic field strength from the synchrotron intensity (Sect. 18.4.1).

Linearly polarized synchrotron emission (examples in Figs. 18.4 and 18.6) emerges from ordered fields in the sky plane. As polarization "vectors" are ambiguous by 180°, they cannot distinguish *regular (coherent) fields*, defined to have a constant direction within the telescope beam, from *anisotropic turbulent fields*,

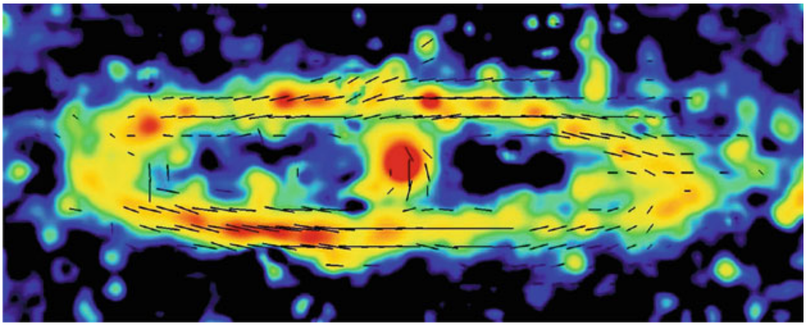

Fig. 18.1 Total radio intensity (colors) and B-vectors (corrected for Faraday rotation) in the Andromeda galaxy (M 31), observed at 6 cm with the Effelsberg telescope (from Berkhuijsen et al. 2003)

which are generated from isotropic turbulent fields by compressing or shearing gas flows and reverse their direction within the telescope beam. Unpolarized synchrotron emission indicates *isotropic turbulent (random) fields* which have random directions in 3-D and have been amplified by turbulent gas flows.

The intrinsic degree of linear polarization of synchrotron emission is about 75%. The observed degree of polarization is smaller due to the contribution of unpolarized thermal emission, which may dominate in star-forming regions, by *Faraday depolarization* along the line of sight and across the beam (Sokoloff et al. 1999), and by geometrical depolarization due to variations of the field orientation within the beam.

The polarization vector is rotated in a magnetized thermal plasma by *Faraday rotation*. As the rotation angle is sensitive to the sign of the field direction, only regular fields give rise to Faraday rotation, while the Faraday rotation contributions of turbulent fields cancel along the line of sight. Measurements of the Faraday rotation from multi-wavelength observations (Figs. 18.15 and 18.16) yield the strength and direction of the average regular field component along the line of sight. If Faraday rotation is small (in galaxies typically at wavelengths shorter than a few centimeters), the B-vector of polarized emission gives the intrinsic field orientation in the sky plane, so that the magnetic pattern can be mapped directly (Beck 2005).

The Faraday rotation angle $\Delta\chi$ is proportional to the square of the wavelength λ and to the *Faraday depth (FD)*,[1] different from the *rotation measure (RM)*.[2] If one or more rotating regions are located in front of the emitting region (*Faraday screen*), *RM* and *FD* are identical. Distinct emitting and rotating regions located along the line of sight generate a spectrum of FD components, and RM varies with λ^2. In such

[1] $FD = 0.81 \int B_{\|}\, n_e\, dl$, where FD is measured in rad m^{-2}, the line-of-sight magnetic field $B_{\|}$ in μG, the thermal electron density n_e in cm^{-3}, and the line of sight l in pc.

[2] RM is the slope of the function $\Delta\chi\,(\lambda^2)$, $RM = \Delta\chi/\Delta\lambda^2$, and hence varies with λ^2 if $\Delta\chi$ is a nonlinear function of λ^2.

cases, multi-channel spectro-polarimetric radio data are needed that can be Fourier-transformed into Faraday space, called *RM Synthesis* (Chap. 3). If the medium has a relatively simple structure, the 3-D structure of the magnetized interstellar medium can be determined (*Faraday tomography*).

A grid of RM measurements of polarized background sources is another powerful tool to study magnetic field patterns in galaxies (Stepanov et al. 2008), but a large number of background sources is required to recognize the field patterns, to separate the Galactic foreground contribution and to account for intrinsic RMs of the background sources.

18.4 Total Magnetic Fields

18.4.1 Field Strengths

The typical average *equipartition strength* of the total magnetic field (Beck and Krause 2005) in spiral galaxies is about $10\,\mu$G, assuming energy equipartition between cosmic rays and magnetic fields. The equipartition assumption is valid on scales of larger than about 1 kpc (Stepanov et al. 2014). Radio-faint galaxies like M 31 (Fig. 18.1) and M 33 have weaker total magnetic fields (about $6\,\mu$G), while gas-rich spiral galaxies with high star-formation rates, like M 51 (Fig. 18.5), M 83 (Fig. 18.6) and NGC 6946, have total field strengths of 20–30 μG in their spiral arms. The strongest total fields of 50–100 μG are found in starburst galaxies, like M 82 (Adebahr et al. 2013) and the "Antennae" NGC 4038/9 (Chyży and Beck 2004), and in nuclear starburst regions, like in NGC 253 (Heesen et al. 2011a), and in barred galaxies (Beck et al. 2005).

If energy losses of cosmic-ray electrons are significant, especially in starburst regions or massive spiral arms, the equipartition values are lower limits (Beck and Krause 2005) and are probably underestimated in starburst galaxies by a factor of a few (Thompson et al. 2006). Field strengths of 0.5–18 mG were detected in starburst galaxies by the Zeeman effect in the OH megamaser emission line at 18 cm wavelength (Robishaw et al. 2008). These values refer to highly compressed gas clouds and are not typical of the diffuse interstellar medium.

The relative importance of various competing forces in the interstellar medium can be estimated by comparing the corresponding *energy densities*. The mean energy densities of the total (mostly turbulent) magnetic field and the cosmic rays in NGC 6946 (Fig. 18.2) and M 33 are $\simeq 10^{-11}\,\mathrm{erg\,cm^{-3}}$ and $\simeq 10^{-12}\,\mathrm{erg\,cm^{-3}}$, respectively (Beck 2007; Tabatabaei et al. 2008), similar to that of the turbulent gas motions across the whole star-forming disk, but about 10 times larger than that of the ionized gas. Magnetic fields are dynamically important. The total magnetic energy density may even dominate in the outer galaxy where the equipartition field strength is an underestimate due to energy losses of the cosmic-ray electrons. The energy density of the regular magnetic field decreases even more slowly than that

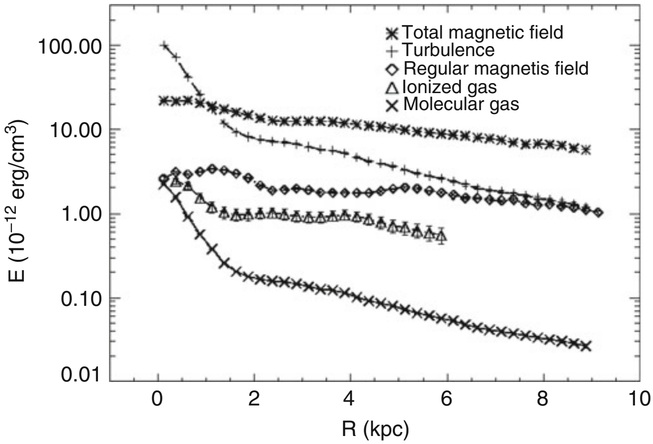

Fig. 18.2 Radial variation of the energy densities in NGC 6946: total magnetic field E_B $(B_t^2/8\pi)$, regular magnetic field $(B_{reg}^2/8\pi)$, turbulent motion of the neutral gas E_{turb} $(0.5\,\rho_n\,v_{turb}^2$, where $v_{turb}\approx 7\,\text{km/s})$, thermal energy of the ionized gas E_{th} $(0.5\,n_e\,k\,T_e)$ and thermal energy of the molecular gas E_n $(0.5\,\rho_n\,k\,T_n)$, determined from observations of synchrotron and thermal radio continuum and the CO and HI line emissions (from Beck 2007)

of the total field. Although the star-formation activity is low in the outer disk, the magneto-rotational instability (MRI) may serve as the source of turbulence required for dynamo action (Sellwood and Balbus 1999; Elstner et al. 2014).

In the case of energy equipartition, the radial scale length of the total field in the disk of mildly inclined galaxies, or the vertical scale height in the halo of edge-on galaxies, is at least $(3-\alpha)$ times larger than the synchrotron scale length of typically 4 kpc (Basu and Roy 2013) (where $\alpha \simeq -1$ is the synchrotron spectral index). The resulting value of $\simeq 16$ kpc is a lower limit because the cosmic-ray electrons lose their energy with distance from the star-forming disk and the equipartition assumption yields too small values for the field strength. The galactic fields probably extend far out into intergalactic space, but at GHz frequencies the measured extent of the radio disks of galaxies is limited by energy loss of cosmic-ray electrons. Measurements at low frequencies (where energy losses are smaller) are needed, e.g. with LOFAR (Chap. 1). Faraday rotation towards polarized background sources may allow us to measure weak fields to even larger distances from the star-forming disks. A large radial scale length may mean that magnetic fields affect the global rotation of the gas in the outer parts of spiral galaxies (Jałocha et al. 2012; Ruiz-Granados et al. 2010), but this cannot explain the flat rotation curves (Elstner et al. 2014).

18.4.2 The Radio–Infrared Correlation

The integrated luminosity of the total radio continuum emission at centimeter wavelengths (frequencies of a few GHz), which is mostly of nonthermal synchrotron origin, and the far-infrared (FIR) luminosity of star-forming galaxies are tightly correlated. This correlation is one of the tightest correlations known in astronomy. It extends over five orders of magnitude (Bell 2003) and is valid in starburst galaxies to redshifts of at least 3 (Seymour et al. 2008). Hence the total radio emission can serve as a tracer of magnetic fields and of star formation out to large distances. The correlation requires that total (mostly turbulent) magnetic fields and star formation are connected, so that the field strength exceeds several 100 μG in distant galaxies (Murphy 2009). The tightness needs multiple feedback mechanisms that are not yet understood (Lacki et al. 2010).

The total radio and far-infrared (FIR) intensities *within* galaxies are also highly correlated. The exponent of the correlation in M 51 was found to be different in the central region, spiral arms and interarm regions (Dumas et al. 2011; Basu et al. 2012). The magnetic field and its structure play an important role to understand the correlation (Tabatabaei et al. 2013a,b). The radio–infrared correlation can be presented as a correlation between turbulent field strength and star-formation rate (Fig. 18.3, Tabatabaei et al. 2013a; Heesen et al. 2014). In contrast, the ordered field is either uncorrelated with the star-formation rate, or anticorrelated in galaxies where the ordered field is strongest in interarm regions with low star formation (Fig. 18.4). A wavelet cross-correlation analysis for M 33 showed that the radio–

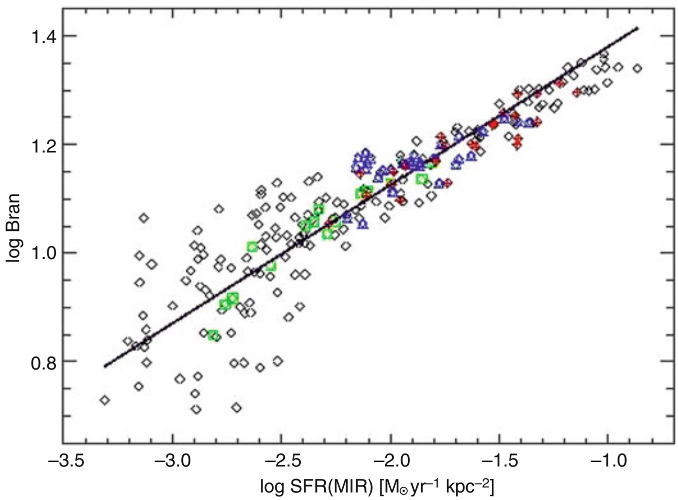

Fig. 18.3 Correlation between the strength of the total equipartition field (dominated by the turbulent field) and star-formation rate per area (determined from the 24 μm infrared intensities) within the galaxy NGC 4254 (from Chyży 2008)

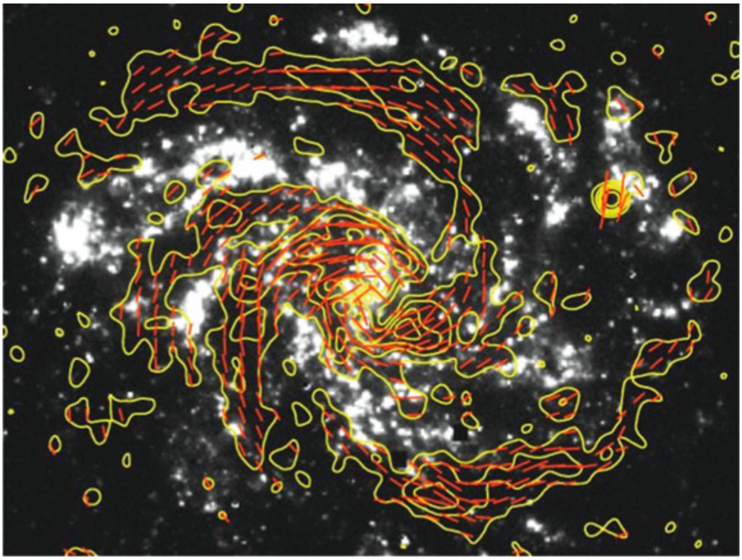

Fig. 18.4 Polarized radio emission (contours) and B-vectors of NCC 6946, combined from observations at 6 cm wavelength with the VLA and Effelsberg telescopes and smoothed to 15″ resolution (from Beck 2007), overlaid onto an Hα image from Anne Ferguson (Copyright: MPIfR Bonn and *Sterne und Weltraum*)

FIR correlation holds at scales <1 kpc (Tabatabaei et al. 2007). The correlation in the Large Magellanic Cloud (LMC) breaks down below scales of about 50 pc (Hughes et al. 2006). The propagation of cosmic-ray electrons away from their sources in star-forming regions is probably responsible for the breakdown scale, and the propagation length depends on the field structure (Tabatabaei et al. 2013b).

18.5 Structure of Ordered Magnetic Fields

18.5.1 Spiral Galaxies

Ordered (regular and/or anisotropic) field traced by polarized synchrotron emission form spiral patterns in almost every galaxy (Beck 2005), even in galaxies with a star-forming ring (Chyży and Buta 2008), in flocculent galaxies without massive spiral arms (Soida et al. 2002), in the central regions of galaxies and in circum-nuclear gas rings of barred galaxies (Beck et al. 2005). Ordered fields are generally strongest (10–15 μG) in the regions *between* the optical spiral arms and oriented parallel to the adjacent spiral arms, in some galaxies forming *magnetic arms*, like in

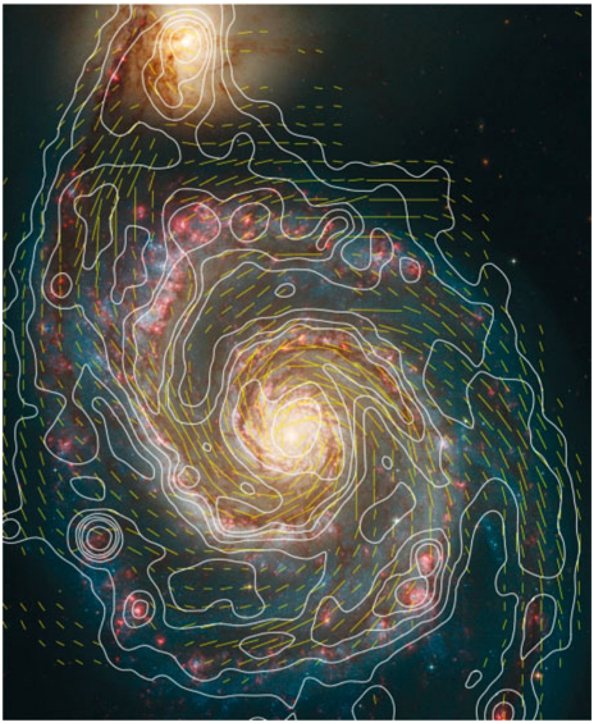

Fig. 18.5 Total radio emission (contours) and B-vectors of M 51, combined from observations at 6 cm wavelength with the VLA and Effelsberg telescopes and smoothed to 15″ resolution (from Fletcher et al. 2011), overlaid onto an optical image from the HST (Copyright: MPIfR Bonn and *Hubble Heritage Team*. Graphics: magazine *Sterne und Weltraum*)

IC 342 (Krause 1993) and NGC 6946 (Fig. 18.4), with exceptionally high degrees of polarization (up to 50%). These are probably generated by a large-scale dynamo (Sect. 18.2). In galaxies with strong density waves like M 51 (Fig. 18.5) and M 83 (Fig. 18.6) enhanced ordered (anisotropic turbulent) fields occur at the inner edges of the inner optical arms, in the interarm regions and in the outer optical arms. From an analysis of dispersions of the radio polarization angles at 6 cm in M 51, the ratio of the correlation lengths parallel and perpendicular to the local ordered magnetic field is about 2 (Houde et al. 2013).

The observed smooth spiral patterns with radially decreasing pitch angles (Fletcher 2010) indicate a general decoupling between magnetic fields and the gas flow, as predicted by $\alpha - \Omega$ dynamo action. At present, no other model can explain the magnetic spiral patterns in the many types of galaxies.

The typical degree of radio polarization within the spiral arms is only a few percent; hence the field in the spiral arms must be mostly tangled or randomly oriented within the telescope beam, the width of which corresponds to a few 100 pc. Turbulent fields in spiral arms are probably generated by turbulent gas motions related to star formation activity (small-scale dynamo).

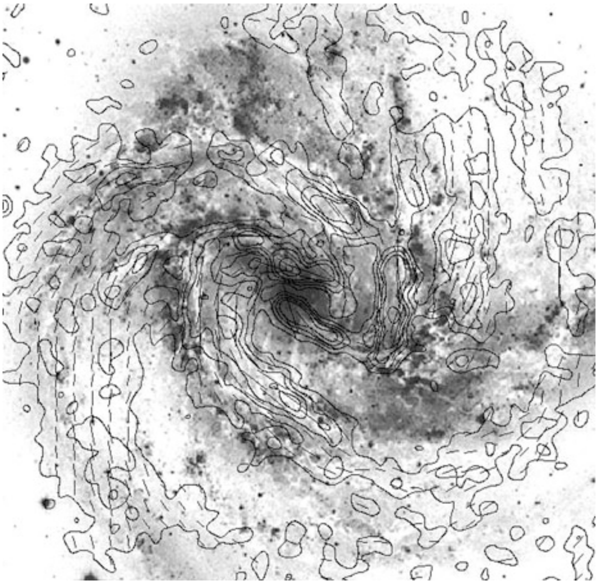

Fig. 18.6 Polarized radio emission (contours) and B-vectors of M 83, combined from observations at 6 cm wavelength with the VLA and Effelsberg telescopes and smoothed to 15″ resolution (from Beck, unpublished), overlaid onto an optical image from Dave Malin, Anglo Australian Observatory (Copyright: MPIfR Bonn and AAO)

At wavelengths of around 20 cm, most of the polarized emission from the far side of the disk and halo is Faraday-depolarized and the emission from the front side dominates. A striking asymmetry of the polarized emission occurs along the major axis of 12 spiral galaxies with inclinations of less than about 60°, observed with sufficiently high sensitivity. The emission is always much weaker around the kinematically receding side (positive radial velocities) of the major axis (Braun et al. 2010; Vollmer et al. 2013). This asymmetry is still visible at 11 cm wavelength, but disappears at smaller wavelengths where the emission from the far side becomes observable. In strongly inclined galaxies, both sides of the major axis become Faraday-depolarized at around 20 cm. Modeling shows that a combination of disk and halo fields, as predicted by $\alpha - \Omega$ dynamo models (Sect. 18.2), can explain the asymmetry (Braun et al. 2010).

18.5.2 Barred Galaxies

In galaxies with massive bars the field lines follow the gas flow (Fig. 18.7). As the gas rotates faster than the bar pattern of a galaxy, a shock occurs in the cold gas, which has a small sound speed, while the flow of warm, diffuse gas is only slightly

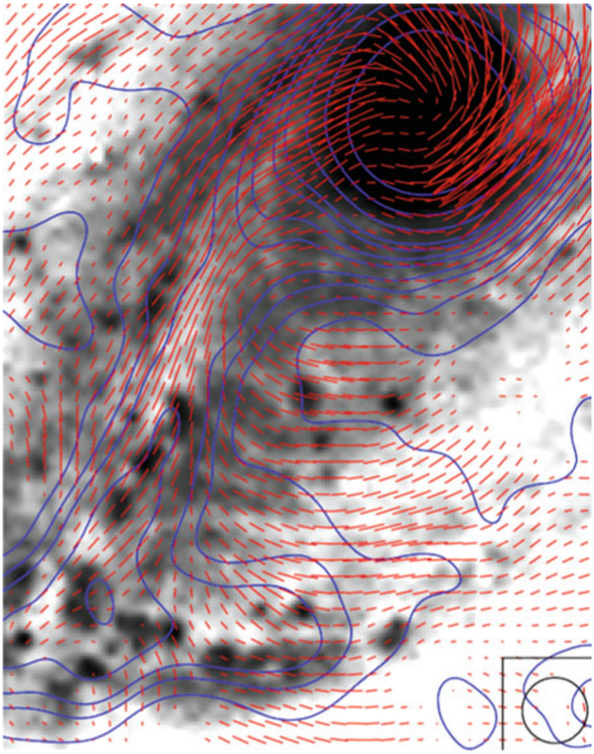

Fig. 18.7 Total radio emission (contours) and B-vectors of the barred galaxy NGC 1097, observed at 6 cm wavelength with the VLA and smoothed to 10″ resolution (from Beck et al. 2005). The background optical image is from Halton Arp (Copyright: MPIfR Bonn and Cerro Tololo Observatory)

compressed but sheared. The ordered field is also hardly compressed, probably coupled to the diffuse gas and strong enough to affect its flow (Beck et al. 2005). The ordered field is also strong in the upstream region (south of the center in Fig. 18.7), oriented almost perpendicular to the bar. The polarization pattern in barred galaxies can be used as a tracer of shearing gas flows in the sky plane and complements spectroscopic measurements of radial velocities.

The central regions of barred galaxies are often sites of ongoing intense star formation and strong magnetic fields that can affect gas flows. NGC 1097 hosts a bright ring with about 1.5 kpc diameter and an active nucleus in its center (Fig. 18.8). The ordered field in the ring has a spiral pattern and extends to the nucleus. The orientation of the innermost spiral field agrees with that of the spiral dust filaments visible on optical images. Magnetic stress in the circumnuclear ring due to the strong total magnetic field (about 50 μG) can drive gas inflow (Balbus and Hawley 1998) at a rate of several solar masses per year, which is sufficient to fuel the activity of the nucleus (Beck et al. 2005).

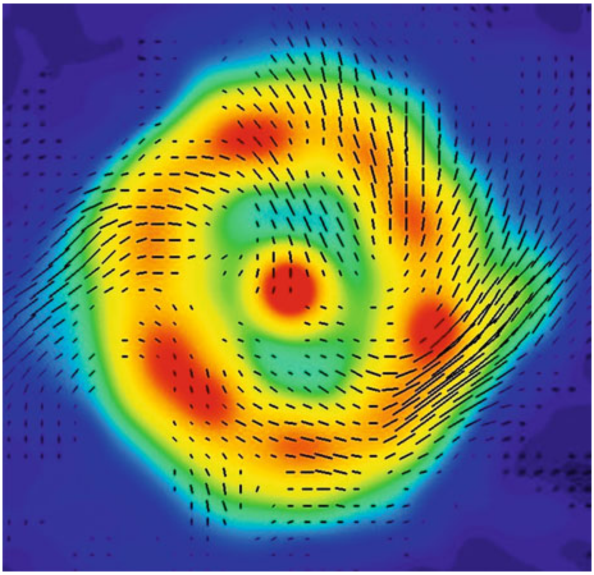

Fig. 18.8 Total radio intensity and B-vectors in the circumnuclear ring of the barred galaxy NGC 1097, observed at 3.5 cm wavelength with the VLA at 3″ resolution (from Beck et al. 2005)

18.5.3 Flocculent and Irregular Galaxies

Flocculent galaxies have disks but no grand-design spiral structure. Nevertheless, spiral magnetic patterns are observed in all flocculent galaxies, indicating that the $\alpha - \Omega$ dynamo works independently of density waves. Ordered magnetic fields with strengths similar to those in grand-design spiral galaxies have been detected in the flocculent galaxies M 33, NGC 3521, NGC 5055 and in NGC 4414 (Soida et al. 2002), and also the mean degree of polarization (corrected for the differences in spatial resolution) is similar in grand-design and flocculent galaxies (Knapik et al. 2000).

Radio continuum maps of irregular, slowly rotating galaxies may reveal strong total magnetic fields, e.g. in the Magellanic-type galaxy NGC 4449 (Fig. 18.9), with a partly ordered field of about 7 μG strength and a spiral pattern (Chyży et al. 2000). Faraday rotation shows that this ordered field is mostly regular and the $\alpha - \Omega$ dynamo is operating. Dwarf irregular galaxies with almost chaotic rotation do not have any regular fields and only spots of faint polarized emission (Heesen et al. 2011b) (see also Fig. 18.10). The turbulent field strengths are generally smaller than in spiral galaxies (Chyży et al. 2011), except for starburst dwarfs, e.g. NGC 1569 with 10–15 μG field strength (Kepley et al. 2010), where star formation activity is sufficiently high for the operation of the small-scale dynamo.

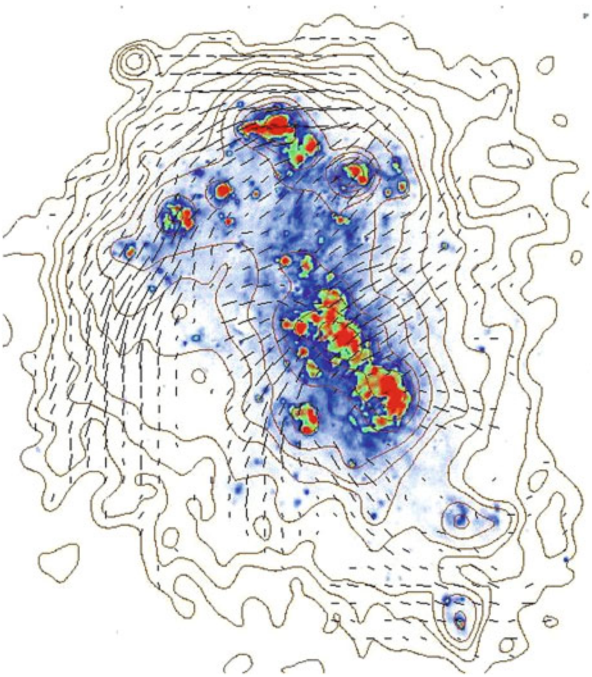

Fig. 18.9 Total radio intensity (contours) and B-vectors of the dwarf irregular galaxy NGC 4449, observed at 3.6 cm with the VLA (from Chyży et al. 2000). The background Hα image is from Dominik Bomans (Bochum University)

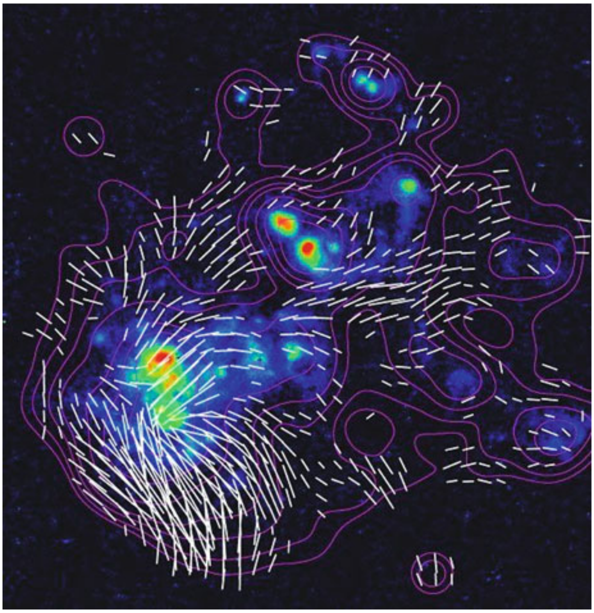

Fig. 18.10 Total radio intensity (contours) and B-vectors of the dwarf irregular galaxy IC 10, observed at 6 cm with the VLA (from Chyży et al., in prep). The background Hα image is from Dominik Bomans (Bochum University)

18.5.4 Interacting Galaxies

Gravitational interaction between galaxies leads to asymmetric gas flows, compression, shear, enhanced turbulence and outflows. Magnetic fields can become aligned along the compression front or perpendicular to the velocity gradients. Such gas flows make turbulent fields highly anisotropic.

The classical interacting galaxy pair is NGC 4038/39, the "Antennae" (Chyży and Beck 2004). It shows bright, extended radio emission filling the whole system. In the interaction region between the galaxies, where star formation did not yet start, and at the northeastern edge of the system, the magnetic field is partly ordered, probably the result of compression and shearing motions along the tidal tail. Particularly strong, almost unpolarized emission comes from a region of violent star formation, hidden in dust. The average total magnetic field is stronger than in normal spirals, but the mean degree of polarization is unusually low, implying that the fields are tangled.

Interaction with a dense intergalactic medium also imprints unique signatures onto magnetic fields and thus the radio emission. The Virgo cluster is a location of especially strong interaction effects (Figs. 18.11 and 18.12), and almost all cluster galaxies observed so far show asymmetries of their polarized emission because the outer magnetic fields were compressed (Vollmer et al. 2007, 2013; Weżgowiec et al. 2007, 2012). Ordered fields are an excellent tracer of past interactions between galaxies or with the intergalactic medium.

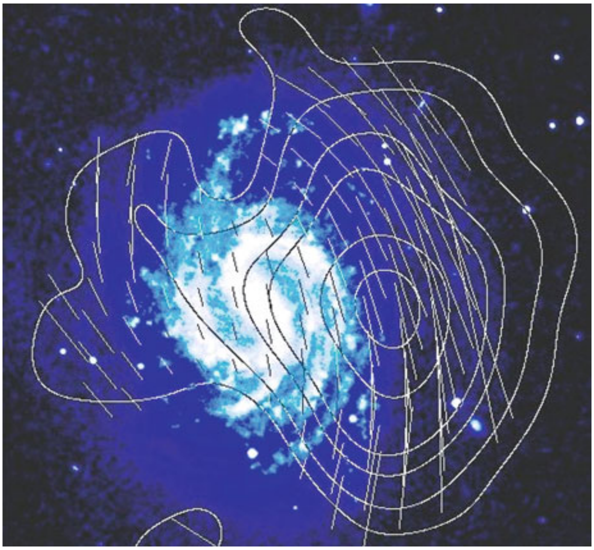

Fig. 18.11 Polarized radio intensity (contours) and B-vectors of the Virgo galaxy NGC 4535, observed at 6 cm with the Effelsberg telescope (from Weżgowiec et al. 2007). The background optical image is from the Digital Sky Survey

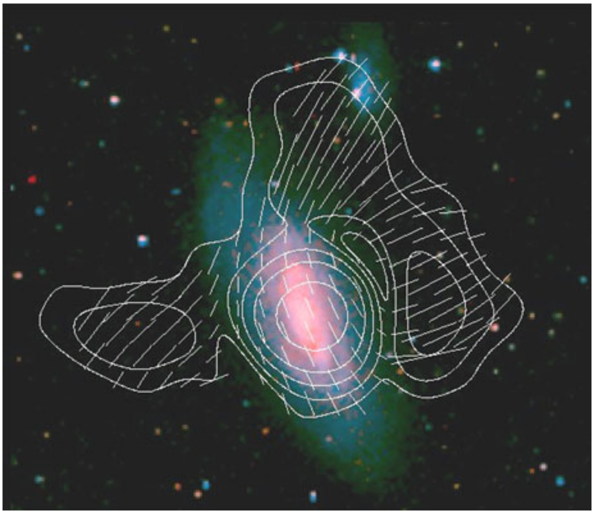

Fig. 18.12 Polarized radio intensity (contours) and B-vectors of the Virgo galaxy NGC 4569, observed at 6 cm with the Effelsberg telescope (from Chyży et al. 2006). The background optical image is from the Digital Sky Survey

18.5.5 Halos Around Edge-on Galaxies

Nearby galaxies seen *edge-on* generally show a disk-parallel field near the disk plane (Dumke et al. 1995). As a result, polarized emission can also be detected from distant, unresolved galaxies if the inclination is larger than about 20° (Stil et al. 2009). This opens a new method to search for ordered fields in distant galaxies. High-sensitivity radio polarization observations of edge-on galaxies like NGC 253 (Heesen et al. 2009b), NGC 891 (Fig. 18.13) and NGC 5775 (Fig. 18.14) revealed vertical field components in the halo forming an X-shaped pattern which may be related to dynamo action (Moss et al. 2010) or to outflows.

The stronger magnetic field in the central regions leads to larger synchrotron loss, leading to the "dumbbell" shape of many radio halos, e.g. in NGC 253 (Heesen et al. 2009a). From the radio scale heights at several frequencies and the corresponding lifetimes of cosmic-ray electrons (due to synchrotron, IC and adiabatic losses) a transport speed of about 300 km/s was measured for the electrons in the halo of NGC 253 (Heesen et al. 2009a). Most edge-on galaxies observed so far have radio scale heights of about 2 kpc. Because the average field strengths and hence electron lifetimes are different in these galaxies, this indicates that the outflow speed of the electrons increases with the average field strength in order to achieve similar scale heights (Krause 2009). The average field strength is related to the average gas density and star-formation rate.

In the exceptionally large radio halos around the irregular and interacting galaxies M 82 (Adebahr et al. 2013; Reuter et al. 1994) and NGC 4631 (Golla and Hummel 1994; Irwin et al. 2012; Mora and Krause 2013) a few magnetic spurs could be resolved, connected to star-forming regions. These observations support the idea of a strong galactic outflow that is driven by regions of star formation in the inner disk.

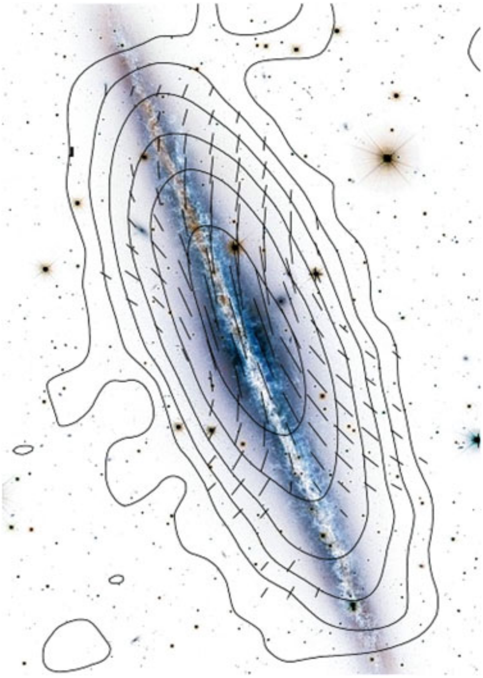

Fig. 18.13 Total radio emission (84″ resolution) and B-vectors of the edge-on galaxy NGC 891, a galaxy similar to the Milky Way, observed at 3.6 cm with the Effelsberg telescope (from Krause 2009). The background optical image is from the CFHT

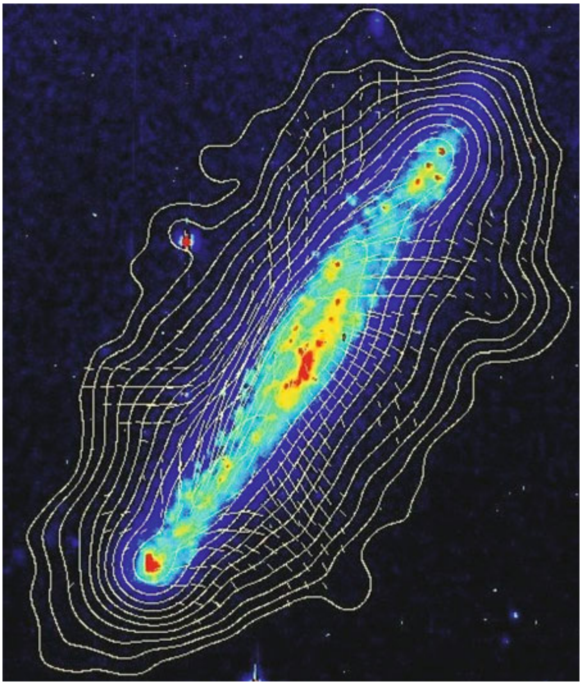

Fig. 18.14 Total radio intensity and B-vectors of the edge-on galaxy NGC 5775, observed at 6 cm wavelength with the VLA at 17″ resolution (from Tüllmann et al. 2000)

18.5.6 Early-Type and Spheroidal Galaxies

Spiral galaxies of type Sa and S0 and elliptical galaxies without an active nucleus have very little star formation and hence hardly produce cosmic rays that could emit synchrotron emission. The only deep observation of a Sa galaxy, M 104 with a prominent dust ring, revealed weak, ordered magnetic fields (Krause et al. 2006). Large-scale regular magnetic fields may exist in differentially rotating galaxies without star formation because turbulence can be generated by the magneto-rotational instability (MRI) (Sellwood and Balbus 1999). Their detection may become possible via RM grids of background sources with future radio telescopes (Chap. 1).

The search for synchrotron emission from nearby dwarf spheroidal galaxies without star formation is an attractive possibility to detect decaying weakly interactive massive particles (WIMPs), candidates of dark matter (Colafrancesco et al. 2007).

18.6 Regular Magnetic Fields

18.6.1 Large-Scale Fields in Galaxy Disks

Spiral fields are generated by compression, by shear in interarm regions, or by dynamo action (Sect. 18.2). Large-scale patterns of Faraday rotation measures (RM) are signatures of regular fields generated by the $\alpha - \Omega$ dynamo and can be identified from diffuse polarized emission of the galaxy disks (Krause 1990) or from RM data of polarized background sources (Stepanov et al. 2008). If several dynamo modes are superimposed, a Fourier analysis of the RM variation with azimuthal angle is needed. The resolution of present-day observations is sufficient to identify 2–3 modes.

The disks of about a dozen nearby spiral galaxies reveal large-scale RM patterns. The Andromeda galaxy M 31 (Fig. 18.1) is the prototype of a dynamo-generated axisymmetric spiral disk field (Fletcher et al. 2004). Other candidates for a dominating axisymmetric disk field (dynamo mode $m = 0$) are the nearby spirals IC 342 (Krause et al. 1989a) and NGC 253 (Heesen et al. 2009b). The axisymmetric field in the irregular Large Magellanic Cloud (LMC) is almost azimuthal (small pitch angle) (Mao et al. 2012). Dominating bisymmetric spiral fields (dynamo mode $m = 1$) are rare, as predicted by dynamo models, but possibly exists in M 81 (Krause et al. 1989b). Faraday rotation in NGC 6946 (Fig. 18.15) and in other similar galaxies with magnetic arms can be described by a superposition of two azimuthal dynamo modes ($m = 0$ and $m = 2$) with about equal amplitudes where the quadrisymmetric ($m = 2$) spiral mode is phase shifted with respect to the density wave (Beck 2007). For several other galaxies, three modes ($m = 0$, 1 and 2) are necessary to describe the data (Fletcher 2010).

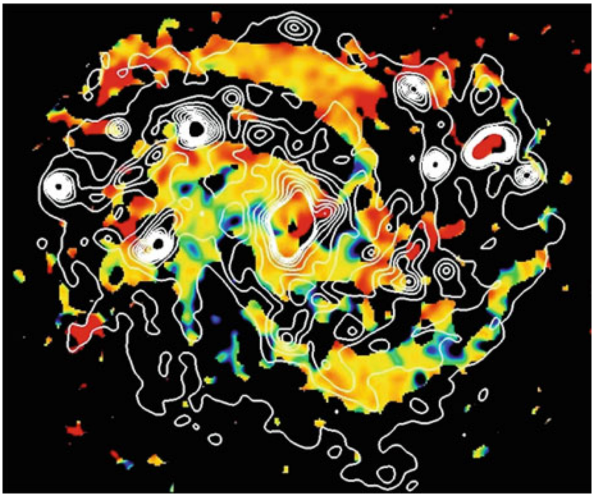

Fig. 18.15 Total radio intensity at 6 cm wavelength (contours) and Faraday rotation measures between 3.6 and 6 cm wavelengths (colors) in NGC 6946, derived from combined observations with the VLA and Effelsberg telescopes at 15″ resolution (from Beck 2007). The color scale ranges from $-75\,\mathrm{rad/m^2}$ to $+175\,\mathrm{rad/m^2}$. The average rotation measure of about $+50\,\mathrm{rad/m^2}$ is caused by the foreground medium in the Milky Way

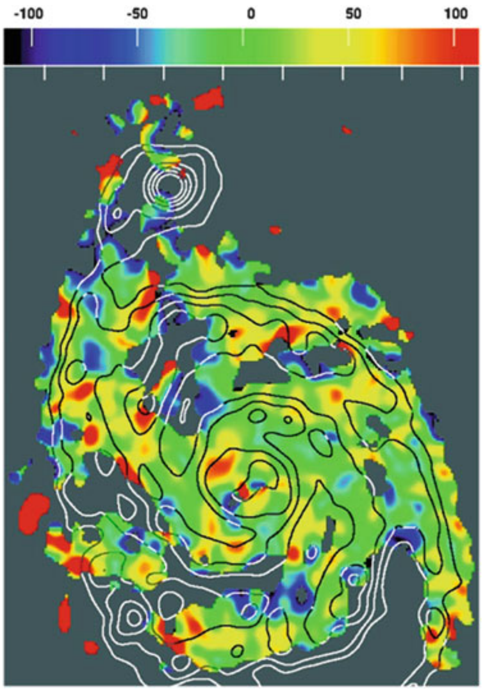

Fig. 18.16 Total radio intensity at 6 cm wavelength (contours) and Faraday rotation measures between 3.6 and 6 cm wavelengths in M 51, derived from combined observations with the VLA and Effelsberg telescopes at 15″ resolution (from Fletcher et al. 2011). The color scale ranges from $-120\,\mathrm{rad/m^2}$ to $+120\,\mathrm{rad/m^2}$

However, the spiral pattern of magnetic fields cannot be solely the result of $\alpha - \Omega$ dynamo action. If the beautiful spiral pattern of M 51 seen in radio polarization (Fig. 18.5) were only due to a regular field in the disk, its line-of sight component should generate a conspicuous large-scale pattern in RM, which is not observed (Fig. 18.16). This means that a large amount of the ordered field is anisotropic turbulent and probably generated by compression and shear of the non-axisymmetric gas flows in the density-wave potential. The anisotropic turbulent field is strongest at the positions of the prominent dust lanes on the inner edge of the inner gas spiral arms, due to compression of turbulent fields in the density-wave shock. Regular fields (dynamo modes $m = 0$ and $m = 2$) also exist in the disk of M 51, but are much weaker than the anisotropic turbulent field (Fletcher et al. 2011).

In the disks of many other galaxies no clear patterns of Faraday rotation were found. Either several high dynamo modes are superimposed and cannot be distinguished with the limited sensitivity and resolution of present-day telescopes, or the timescale for the generation of large-scale modes is longer than the galaxy's lifetime (Arshakian et al. 2009), or field injection by strong star-formation activity perturbs the generation of the large-scale regular field (Moss et al. 2012).

By comparing the signs of the RM distribution and the velocity field on both sides of a galaxy's major axis, the inward and outward directions of the radial component of the axisymmetric spiral field can be distinguished (Krause and Beck 1998). Dynamo models predict that both signs have the same probability, which is confirmed by observations. The axisymmetric fields of M 31, IC 342, NGC 253 and the axisymmetric field component in NGC 6946 point inwards, while those of NGC 4254, NGC 5775 and the axisymmetric component of the disk field in M 51 point outwards.

18.6.2 Large-Scale Fields in Galaxy Halos

While the azimuthal symmetry of the magnetic field is known for many galaxies, the vertical symmetry (even or odd) is harder to determine. The field of odd symmetry reverses its sign above and below the galactic plane. In mildly inclined galaxies the RM patterns of diffuse polarized emission from even and odd-symmetry fields are similar, while the RMs of background sources are different: strong for odd and small for even symmetry. Background RMs in the Large Magellanic Cloud field indicate an even-symmetry field (Mao et al. 2012). The symmetry type is best visible in strongly inclined galaxies, via the RM sign above and below the plane. Indication for an even-symmetry field was found in NGC 253 (Heesen et al. 2009b).

With help of high-resolution RM mapping, an outwards-directed helical field of about 20 μG strength, extending to at least 1 kpc height, could be identified in the gas outflow cone of NGC 253 (Heesen et al. 2011a). This field may help to confine the outflow.

18.6.3 Field Reversals

Large-scale field reversals at certain radial distances from a galaxy's center, like that observed in the Milky Way (Van Eck et al. 2011; Chap. 17), have not

Table 18.1 Typical field structures in nearby galaxies (where "turbulent" means "isotropic turbulent")

Galaxy type	Magnetic field structure	Regular (dynamo) field
Sc galaxy with strong density wave	Ordered spiral field at inner arm edge and in interarm regions, turbulent field in arms	Moderate
Sb or Sc galaxy with weak or moderate density wave	Ordered spiral field in interarm regions, turbulent + ordered field in arms	Strong
Barred Sc galaxy	Ordered + turbulent field along bar, spiral field outside bar	Moderate
Flocculent Sc or Sd galaxy	Spiral + turbulent field in disk	Weak
Irregular galaxy	Turbulent field in star-forming regions + segments of ordered field	Weak
Starburst dwarf galaxy	Turbulent field in star-forming regions	Not detected
Spheroidal dwarf galaxy	Not detected	Not detected
Sa galaxy	Ordered + turbulent fields	Not detected
S0 galaxy	Not detected	Not detected
E galaxy (non-active nucleus)	Not detected	Not detected

been detected in external galaxies, although high-resolution RM maps of Faraday rotation are available for many spiral galaxies. In M 81 the dominating bisymmetric spiral field implies two large-scale reversals (Krause et al. 1989b). In the barred galaxy NGC 7479, where a jet serves as a bright polarized background and where high-resolution observations were possible with high signal-to-noise ratio, several reversals on 1–2 kpc scale were detected in the foreground disk of the galaxy (Laine and Beck 2008). A field reversal extending over 0.6 kpc scale and coinciding with a hole in neutral hydrogen was detected in NGC 6946 (Heald 2012).

The typical magnetic field structures observed in nearby galaxies are summarized in Table 18.1.

18.7 Outlook

Future high-resolution, high-sensitivity observations at medium and high frequencies with the *Jansky Very Large Array* (JVLA) and the planned *Square Kilometre Array* (SKA) (Chap. 1) will directly map the detailed field structure in galaxies and the interaction with the gas. The recently opened low-frequency radio telescope *Low Frequency Array* (LOFAR) and the *Murchison Widefield Array* (MWA) are suitable instruments to search for extended synchrotron radiation at the lowest possible levels in outer galaxy disks and halos and the transition to intergalactic space. We are entering a golden era of magnetic field observations in galaxies.

References

Abreu, P.: The Pierre Auger Collaboration. Astroparticle Phys. **34**, 314 (2010)
Adebahr, B., Krause, M., Klein, U., et al.: Astron. Astrophys. **555**, A23 (2013)
Arshakian, T.G., Beck, R., Krause, M., Sokoloff, D.: Astron. Astrophys. **494**, 21 (2009)
Balbus, S.A., Hawley, J.F.: Rev. Mod. Phys. **70**, 1 (1998)
Basu, A., Roy, S.: Mon. Notices R. Astron. Soc. **433**, 1675 (2013)
Basu, A., Roy, S., Mitra, D.: Astrophys. J. **756**, 141 (2012)
Beck, R.: In: Wielebinski, R., Beck, R. (eds.) Cosmic Magnetic Fields, p. 41. Springer, Berlin (2005)
Beck, R.: Astron. Astrophys. **470**, 539 (2007)
Beck, R., Brandenburg, A., Moss, D., Shukurov, A., Sokoloff, D.: Ann. Rev. Astron. Astrophys. **34**, 155 (1996)
Beck, R., Krause, M.: Astron. Nachr. **326**, 414 (2005)
Beck, R., Fletcher, A., Shukurov, A., et al.: Astron. Astrophys. **444**, 739 (2005)
Bell, E.F.: Astrophys. J. **586**, 794 (2003)
Berkhuijsen, E.M., Beck, R., Hoernes, P.: Astron. Astrophys. **398**, 937 (2003)
Braun, R., Heald, G., Beck, R.: Astron. Astrophys. **514**, A42 (2010)
Caprini, C., Durrer, R., Fenu, E.: J. Cosmol. Astroparticle Phys. **11**, 001 (2009)
Chyży, K.T.: Astron. Astrophys. **482**, 755 (2008)
Chyży, K.T., Beck, R.: Astron. Astrophys. **417**, 541 (2004)
Chyży, K.T., Buta, R.J.: Astrophys. J. **677**, L17 (2008)
Chyży, K.T., Beck, R., Kohle, S., Klein, U., Urbanik, M.: Astron. Astrophys. **356**, 757 (2000)
Chyży, K.T., Soida, M., Bomans, D.J., et al.: Astron. Astrophys. **447**, 465 (2006)
Chyży, K.T., Weżgowiec, M., Beck, R., Bomans, D.J.: Astron. Astrophys. **529**, A94 (2011)
Colafrancesco, S., Profumo, S., Ullio, P.: Phys. Rev. D **75**, 023513 (2007)
Crutcher, R.M., Wandelt, B., Heiles, C., Falgarone, E., Troland, T.H.: Astrophys. J. **725**, 466 (2010)
Dolag, K., Kachelriess, M., Ostapchenko, S., Tomas, R.: Astrophys. J. **727**, L4 (2011)
Dumas, G., Schinnerer, E., Tabatabaei, F.S., et al.: Astron. J. **141**, 41 (2011)
Dumke, M., Krause, M., Wielebinski, R., Klein, U.: Astron. Astrophys. **302**, 691 (1995)
Elstner, D., Beck, R., Gressel, O.: Astron. Astrophys. **568**, A104 (2014)
Fletcher, A.: In: Kothes, R., et al. (eds.) The Dynamic Interstellar Medium. ASP Conference Series, vol. 438, p. 197. Astr. Soc. of the Pacific, San Francisco (2010)
Fletcher, A., Berkhuijsen, E.M., Beck, R., Shukurov, A.: Astron. Astrophys. **414**, 53 (2004)
Fletcher, A., Beck, R., Shukurov, A., Berkhuijsen, E.M., Horellou, C.: Mon. Notices R. Astron. Soc. **412**, 2396 (2011)
Fosalba, P., Lazarian, A., Prunet, S., Tauber, J.A.: Astrophys. J. **546**, 762 (2002)
Gent, F.A., Shukurov, A., Sarson, G.R., Fletcher, A., Mantere, M.J.: Mon. Notices R. Astron. Soc. **430**, L40 (2013)
Gissinger, C., Fromang, S., Dormy, E.: Mon. Notices R. Astron. Soc. **394**, L84 (2009)
Golla, G., Hummel, E.: Astron. Astrophys. **284**, 777 (1994)
Greaves, J.S., Holland, W.S., Jenness, T., Hawarden, T.G.: Nature **404**, 732 (2000)
Gressel, O., Elstner, D., Ziegler, U., Rüdiger, G.: Astron. Astrophys. **486**, L35 (2008)
Hanasz, M., Wóltański, D., Kowalik, K.: Astrophys. J. **706**, L155 (2009)
Hanayama, H., Takahashi, K., Kotake, K., et al.: Astrophys. J. **633**, 941 (2005)
Heald, G.: Astrophys. J. **754**, L35 (2012)
Heesen, V., Beck, R., Krause, M., Dettmar, R.-J.: Astron. Astrophys. **494**, 563 (2009a)
Heesen, V., Krause, M., Beck, R., Dettmar, R.-J.: Astron. Astrophys. **506**, 1123 (2009b)
Heesen, V., Beck, R., Krause, M., Dettmar, R.-J.: Astron. Astrophys. **535**, A79 (2011a)
Heesen, V., Rau, U., Rupen, M.P., Brinks, E., Hunter, D.A.: Astrophys. J. **739**, L23 (2011b)
Heesen, V., Brinks, E., Leroy, A.K., et al.: Astron. J. **147**, 103 (2014)
Houde, M., Fletcher, A., Beck, R., et al.: Astrophys. J. **766**, 49 (2013)
Hughes, A., Wong, T., Ekers, R., et al.: Mon. Notices R. Astron. Soc. **370**, 363 (2006)

Irwin, J., Beck, R., Benjamin, R.A., et al.: Astrophys. J. **144**, 44 (2012)
Jałocha, J., Bratek, Ł., Pękala, J., Kutschera, M.: Mon. Notices R. Astron. Soc. **421**, 2155 (2012)
Kepley, A.A., Mühle, S., Everett, J., et al.: Astrophys. J. **712**, 536 (2010)
Knapik, J., Soida, M., Dettmar, R.-J., Beck, R., Urbanik, M.: Astron. Astrophys. **362**, 910 (2000)
Krause, M.: In: Beck, R., et al. (eds.) Galactic and Intergalactic Magnetic Fields, p. 187. Kluwer, Dordrecht (1990)
Krause, M.: In: Krause, F., et al. (eds.) The Cosmic Dynamo, p. 303. Kluwer, Dordrecht (1993)
Krause, M.: Rev. Mex. AyA **36**, 25 (2009)
Krause, F., Beck, R.: Astron. Astrophys. **335**, 789 (1998)
Krause, M., Hummel, E., Beck, R.: Astron. Astrophys. **217**, 4 (1989a)
Krause, M., Beck, R., Hummel, E.: Astron. Astrophys. **217**, 17 (1989b)
Krause, M., Wielebinski, R., Dumke, M.: Astron. Astrophys. **448**, 133 (2006)
Lacki, B.C., Thompson, T.A., Quataert, E.: Astrophys. J. **717**, 1 (2010)
Laine, S., Beck, R.: Astrophys. J. **673**, 128 (2008)
Lazar, M., Schlickeiser, R., Wielebinski, R., Poedts, S.: Astrophys. J. **693**, 1133 (2009)
Mao, S.A., McClure-Griffiths, N.M., Gaensler, B.M., et al.: Astrophys. J. **759**, 25 (2012)
Mora, S.C., Krause, M.: Astron. Astrophys. **560**, A42 (2013)
Moss, D., Sokoloff, D., Beck, R., Krause, M.: Astron. Astrophys. **512**, A61 (2010)
Moss, D., Stepanov, R., Arshakian, T.G., et al.: Astron. Astrophys. **537**, A68 (2012)
Murphy, E.: Astrophys. J. **706**, 482 (2009)
Rees, M.J.: In: Wielebinski, R., Beck, R. (eds.) Cosmic Magnetic Fields, p. 1. Springer, Berlin (2005)
Reuter, H.-P., Klein, U., Lesch, H., Wielebinski, R., Kronberg, P.P.: Astron. Astrophys. **282**, 724 (1994)
Robishaw, T., Quataert, E., Heiles, C.: Astrophys. J. **680**, 981 (2008)
Ruiz-Granados, B., Rubiño-Martín, J.A., Florido, E., Battaner, E.: Astrophys. J. **723**, L44 (2010)
Scarrott, S.M., Ward-Thompson, D., Warren-Smith, R.F.: Mon. Notices R. Astron. Soc. **224**, 299 (1987)
Schleicher, D.R.G., Banerjee, R., Sur, S., et al.: Astron. Astrophys. **522**, A115 (2010)
Schlickeiser, R.: Phys. Rev. Lett. **109**, 261101 (2012)
Sellwood, J.A., Balbus, S.A.: Astrophys. J. **511**, 660 (1999)
Seymour, N., Dwelly, T., Moss, D., et al.: Mon. Notices R. Astron. Soc. **386**, 1695 (2008)
Shukurov, A., Sokoloff, D., Subramanian, K., Brandenburg, A.: Astron. Astrophys. **448**, L33 (2006)
Soida, M., Beck, R., Urbanik, M., Braine, J.: Astron. Astrophys. **394**, 47 (2002)
Sokoloff, D., Bykov, A.A., Shukurov, A., et al.: Mon. Notices R. Astron. Soc. **299**, 189 (1998). Erratum in Mon. Notices R. Astron. Soc. **303**, 207 (1999)
Stepanov, R., Arshakian, T.G., Beck, R., Frick, P., Krause, M.: Astron. Astrophys. **480**, 45 (2008)
Stepanov, R., Shukurov, A., Fletcher, A., et al.: Mon. Notices R. Astron. Soc. **437**, 2201 (2014)
Stil, J.M., Krause, M., Beck, R., Taylor, A.R.: Astrophys. J. **693**, 1392 (2009)
Tabatabaei, F., Beck, R., Krause, M., et al.: Astron. Astrophys. **466**, 509 (2007)
Tabatabaei, F., Krause, M., Fletcher, A., Beck, R.: Astron. Astrophys. **490**, 1005 (2008)
Tabatabaei, F.S., Schinnerer, E., Murphy, E.J., et al.: Astron. Astrophys. **552**, A19 (2013a)
Tabatabaei, F.S., Berkhuijsen, E.M., Frick, P., Beck, R., Schinnerer, E.: Astron. Astrophys. **557**, A129 (2013b)
Thompson, T.A., Quataert, E., Waxman, E., Murray, N., Martin, C.L.: Astrophys. J. **645**, 186 (2006)
Tüllmann, R., Dettmar, R.-J., Soida, M., Urbanik, M., Rossa, J.: Astron. Astrophys. **364**, L36 (2000)
Van Eck, C.L., Brown, J.C., Stil, J.M., et al.: Astrophys. J. **728**, 97 (2011)
Vollmer, B., Soida, M., Beck, R., et al.: Astron. Astrophys. **464**, L37 (2007)
Vollmer, B., Soida, M., Beck, R., et al.: Astron. Astrophys. **553**, A116 (2013)
Weżgowiec, M., Urbanik, M., Vollmer, B., et al.: Astron. Astrophys. **471**, 93 (2007)
Weżgowiec, M., Urbanik, M., Beck, R., et al.: Astron. Astrophys. **545**, A69 (2012)
Widrow, L.M.: Rev. Mod. Phys. **74**, 775 (2002)